

Direct Measurement of Light and Heavy Antibody Chains Using Differential Ion Mobility Spectrometry and Middle-Down Mass Spectrometry

Rafael D Melani^a; Kristina Srzentic^b; Vincent R Gerbasi^a; John P McGee^a; Romain Huguet^c;
Luca Fornelli^d; and Neil L Kelleher^{a*}

^a*Departments of Chemistry, Molecular Biosciences, and Chemical and Biological Engineering; the Chemistry of Life Processes Institute; and the Proteomics Center of Excellence, Northwestern University, Evanston, IL, 60208, United States.*

^b*Thermo Fisher Scientific, Cambridge, MA, 02139, United States.*

^c*Thermo Fisher Scientific, San Jose, CA, 95134, United States.*

^d*Department of Biology, Oklahoma University, Norman, OK, 73019, United States.*

*Contact: Neil L Kelleher, e-mail: n-kelleher@northwestern.edu, address: 2-100 Hogan Hall, 2205 Tech Drive, Evanston, IL, 60208, United States, telephone: +1 847 467-4362.

Short Communication

Abstract

The analysis of monoclonal antibodies (mAbs) by a middle-down approach is a growing field that attracts the attention of many researchers and biopharma companies.

Usually, liquid fractionation techniques are used to separate mAbs polypeptides chains before mass spectrometry (MS) analysis. Gas-phase fractionation techniques such as high-field asymmetric waveform ion mobility spectrometry (FAIMS) can replace liquid-based separations and reduce both analysis time and cost. Here, we present a rapid FAIMS tandem MS method capable of characterizing the polypeptide sequence of mAbs light (Lc) and heavy (Hc) chains in an unprecedented, easy, and fast fashion. This new method uses commercially available instruments and takes ~24 minutes —40-60% faster than regular LC-MS/MS analysis — to acquire fragmentation data using different dissociation methods.

Keywords

FAIMS, Gas-phase Fractionation, Light and Heavy Chains, mAb, Middle-Down Analysis,

Main Text

Monoclonal antibodies (mAbs) based on immunoglobulins G (IgGs) are multichain glycoproteins with an approximate molecular weight of 150 kDa. They consist of four polypeptide chains: two light chains (Lc) of ~25 kDa each and two heavy chains (Hc) of ~50 kDa each, all linked together by disulfide bonds¹. mAbs are the fastest growing class of human therapeutics; the FDA has already approved over 80 therapeutic mAbs since 2018², and they are being used in the treatment of diseases related to cardiovascular, respiratory, hematology, kidney, immunology, and oncology systems^{3;4}. As with any other therapeutic, mAbs are required to have their structure well-characterized to ensure drug safety, efficiency, batch-to-batch consistency, and stability over time⁵.

Bottom-up, middle-down, and top-down mass spectrometry (MS) strategies are often used to fulfill and streamline molecular characterization requirements¹. Bottom-up approaches digest the mAb into peptides before analysis⁶, top-down MS methods analyze intact molecules⁷⁻¹⁰, and middle-down methods are performed by measuring the mass and subsequent fragmenting large pieces or subunits from mAbs (typically 25-50 kDa) that are more suitable for state-of-the-art liquid chromatography tandem mass spectrometry (LC-MS/MS) methods and techniques¹¹⁻¹⁶. The subunits or parts of the polypeptide chain can be obtained through the chemical reduction of disulfide bonds—yielding free Lc and Hc¹⁷—and/or by using a specific enzymatic proteolysis (i.e. digestion with IdeS or IdeZ) that usually generates F(ab')₂ (~100 kDa) and Fc (~50 kDa) pieces¹⁸. The S-S bounds in these pieces can be further reduced, resulting in three ~25 kDa subunits: one Lc and two portions of Hc named Fc/2 and Fd¹⁹.

Even the simplest mixture of two unique polypeptide chains obtainable via disulfide bond reduction (i.e., without proteolysis), Lc and Hc, cannot be analyzed effectively by MS without some type of front-end fractionation that can isolate or partially separate the chains. Both the overlap of their charge state envelopes and ionization suppression effects can lower their spectral signal-to-noise ratio (S/N)—particularly for the larger Hc—and could result in co-isolation during fragmentation experiments (tandem MS, or MS/MS). Fractionation methods are typically based on liquid chromatography performed using reverse phase (RP)¹⁷, size exclusion (SEC)^{20; 21}, or ion exchange (IEX)^{22; 23} columns. Each LC-MS/MS run takes several minutes, generally only one fragmentation method is used per run, and multiple injections are needed to maximize sequence coverage¹⁴. Furthermore, liquid chromatography instruments add expense, with elevated operational costs depending on columns and extent of method development required. Front-end separation based on liquid chromatography also

raise issues of sample carryover, contamination, and potential sample losses via irreversible adsorption.

In sharp contrast to liquid-phase separation, a new high-field asymmetric waveform ion mobility spectrometry (FAIMS) device with cylindrical electrodes and improved transmission has recently been described and allows for rapid and effective gas-phase separation of molecules after they are ionized and prior to the mass spectrometer entrance²⁴;²⁵. FAIMS devices operate at atmospheric pressure, conducting ions among an inner and an outer electrode under a high or low electric field²⁶. The electric fields are generated from an asymmetric waveform, and the ion separation is based on ion differential mobility. Ions with moderate to no difference in mobility between the high and low fields are conducted to the MS, while ions with a large mobility difference are deflected to the electrodes and are lost. Adding a direct current (DC) voltage—termed the compensation voltage (CV)—to the system alters ion trajectories, which provides a compensation for the drift of specific ions and permits those ions to pass through the electrodes and be analyzed^{27; 28}. Ions above ~30 kDa show a strong increase of mobility at high fields, which agrees with expected ion dipole alignment and expands the useful FAIMS separation power²⁹⁻³¹. Summarizing, changes in CV will favor different groups of ions and function as a filter, as observed for peptides³² and proteins²⁹. The use of gas-phase fractionation can exclude the liquid separation step for middle-down mAb analysis, making it fast, less expensive, and more robust.

Herein, we present a novel method for fast middle-down analysis of reduced Lc and Hc chains of mAbs without liquid phase pre-fractionation, using only FAIMS Pro™ coupled to an Orbitrap Eclipse™ Tribrid™ mass spectrometer (FAIMS-MS/MS) capable of performing multiple ion fragmentation techniques.

NIST Monoclonal Antibody Reference Material 8671 (NIST), 300 μg , was denatured in 6 M guanidium chloride and reduced using 30 mM tris(2-carboxyethyl)phosphine hydrochloride (TCEP-HCl) for 90 minutes at 37 °C under agitation. The sample was desalted using 3 kDa molecular weight cut-off Amicon Ultra-0.5 (Millipore Sigma), and the solution was buffer exchanged to Optima LC/MS grade water (Fisher Scientific) for over 10 cycles in a refrigerated centrifuge at 4 °C applying 8,000 $\times g$. Reduced polypeptide chains were resuspended in 50% acetonitrile containing 0.4% of formic acid for an $\sim 2 \mu\text{M}$ final concentration.

The polypeptide mixture was sprayed using a Nanospray FlexTM static source (Thermo Fisher Scientific) and medium-length borosilicate-coated emitters (Thermo Fisher Scientific) on an Orbitrap EclipseTM TribridTM (Thermo Fisher Scientific) equipped with FAIMS ProTM (Thermo Fisher Scientific). The spray voltage was set between 1.5-2.5 kV, and for MS experiments the acquisition range was set between m/z 800-2,000 using a resolving power of 7,500 (at m/z 200), 2 microscans/spectrum, an average of 20 spectra, 100 ms of maximum injection time, automatic gain control (AGC) target of 5×10^5 charges, and source collision-induced dissociation (CID) of 10 V; the instrument was operated in “intact protein” mode (pressure of 2 mTorr). FAIMS ProTM was run at a N₂ carrier gas flow of 0 L/min, an inner electrode temperature of 100 °C, an outer electrode temperature of 100 °C, a dispersion voltage (DV) of -5,000 V for the asymmetric waveform, an entrance plate voltage of 250 V, and the CV was ranging from -30 to +40 V in 10 V steps.

MS/MS experiments for Lc were carried out at FAIMS CV -20 V using the following parameters: 2 microscans/spectrum, resolving power 120,000 (at m/z 200), source CID of 10 V, isolation window of 20 Th centered at m/z 1,102 (charge state +21), maximum injection time of 100 ms, AGC target of 5×10^6 charges, acquisition range set between m/z 500-2,000, average of 20 spectra, and ion transfer tube temperature set at 300 °C. For higher-energy

collisional dissociation (HCD) normalized collision energy (NCE) was set at 10% for charge state 1, CID NCE at 25% for charge state 1, ultraviolet photodissociation (UVPD) was performed using a 213 nm laser and irradiation time of 70 ms, electron transfer dissociation (ETD) AGC target value for fluoranthene radical anions was set to $7-8 \times 10^5$ charges, default charge state of 3, and ETD reaction times of 5 and 7 ms.

MS/MS experiments for Hc were carried out at FAIMS CV +40 V using the following parameters: 1 microscan/spectrum, resolving power 60,000 of (at m/z 200), source CID of 20 V, isolation window of 100 Th centered at m/z 1,000 or 1,200 (charge states +49-53 or +41-44 respectively), maximum injection time of 100 ms, AGC target of 5×10^6 charges, acquisition range set between m/z 500-2,000, average of 20 spectra, ion transfer tube temperature set at 300 °C; for HCD, NCE was set at 15% for charge state 1; CID was performed using 10% of NCE for charge state 1; ETD AGC target value for fluoranthene radical anions was set to $7-8 \times 10^5$ charges, default charge state of 3, using ETD reaction times of 2, 5, and 10 ms; electron-transfer/higher-energy collision dissociation (EThcD) was performed using the same ETD conditions with 2 ms reaction time and 15% of NCE for HCD at charge state 1.

The data were analyzed using Thermo XCalibur Qual Browser v4.0.27.10 (Thermo Fisher Scientific) to average spectra and manipulate .raw files. Mass deconvolution of low-resolution data was performed on UniDec GUI v3.0.0³³. Fragmentation peak fitting and annotation was performed with TDValidator v1.0¹⁴ (Proteinaceous) using the following parameters: signal to noise (S/N) cutoff of 20 for Lc and 2 for Hc data, max ppm tolerance 20 ppm, sub ppm tolerance 15 ppm, cluster tolerance 0.35, minimum score of 0.7, charge range 1-15, and distribution generator Mercury7. S/N was calculated according to the expression: $S/N = (S - B) / (N - B)$ where S is the signal intensity, B is the spectrum base line intensity, and N is the spectrum noise intensity.

A mixture of reduced Lc and Hc, from NIST mAb reference material, was directly sprayed into an Orbitrap Eclipse™ Tribrid™ mass spectrometer, and the obtained MS spectrum is dominated by the charge state envelope of the Lc with the Hc charge state distribution below 20% of relative intensity (Figure 1A). The constitutional ratio between Lc and Hc for NIST mAb is 1:1. However, S/N for Lc was 119 (m/z 1,052, charge state +22), and for Hc it was 14.4 (m/z 1,043, charge state +49) and signal intensities were not equivalent. The lower signal and S/N observed for Hc is due to the signal splitting into more charge states than Lc, the presence of more proteoforms (glycosylation), and differences in ionization efficiency. The deconvoluted spectrum (Figure 1B) confirms the abundance discrepancy with Lc representing ~90% of peak intensities while Hc only ~10%. Looking at Hc proteoforms, G1F was the most intense glycoform observed, G0F represented one third of its intensity, and no other Hc glycoform masses were detected.

Spraying the same mixture into the instrument equipped with FAIMS Pro™ and stepping the compensation voltage (CV) by 10 V from -30 V to +40 V allowed the gas-phase separation of Lc and Hc based on their ion mobilities across the generated high field asymmetric waveforms (Supplementary Figures S1 and S2). Acquisition was performed for three minutes in each CV 10 V steps, and the -20 V step presented the clearest spectrum for Lc (Figure 1C). The most abundant charge state showed a S/N of 2,390 for m/z 1,052 (charge state +22), which is equal to an increase of 20-fold compared to the no FAIMS spectrum. Moreover, the Hc charge distribution observed was below 3% of total ion relative intensity. The deconvoluted spectra is composed of 95.2% of Lc and 4.8% of Hc based on peak intensities (Figure 1D), and the Lc observed average mass of 23,127.31 Da is -11.2 ppm off the theoretical mass 23,127.57 Da. Adducts of sodium (22 Da), guanidine (60 Da), their combination, and the double guanidine species were also observed as well as a 162 Da mass shift which corresponds to the addition of one hexose (Hex) to Lc (Figure 2A). The non-

enzymatic, but covalent adduction of a Hex sugar molecule on a lysine or on a protein N-terminus is called “glycation”, and for the Lc of NIST mAb there are 22 distinct glycosylated peptides reported³⁴. Lc+Hex is reported as trace level post-translational modifications (PTMs)³⁵. In addition, the glycosylated Lc proteoforms correspond to ~4% of the total ion intensity of the non-modified Lc, indicating that FAIMS-MS is suitable to detect low stoichiometry mAbs PTMs.

On the other hand, the CV of +40 V generated the cleanest spectrum for Hc (Figure 1E) with no detection of Lc and a S/N of 477 for m/z 1,043 (charge state +49), which corresponds to a 34-fold increase compared to the spectrum recorded without FAIMS. The observed deconvoluted average mass for Hc G1F was 51,068.59 Da, -10.4 ppm off from the theoretical mass 51,069.12 Da. In the deconvoluted spectrum only Hc was detected (Figure 1F), and it presented 6 glycoforms (Figure 2B): G0F-GlcNAc, G0F, G1F, G2F, G2F+Hex, and G2F+2Hex. Their relative abundances based on ion intensity are 1.5%, 40.5%, 43.6%, 11.8%, 2.1%, and 0.5% respectively. Single- and double-guanidine (60 Da) adducts were also observed. The observed ratios of the glycoforms are in accordance with the literature findings^{36, 37}. As G0F-GlcNAc, G2F+Hex, and G2F+2Hex were just not seen without the use of FAIMS due to their low abundance. Their detection and accurate relative quantitation using FAIMS are a good indicator of the heightened sensitivity afforded using FAIMS-MS.

Preventing the overlap of Lc and Hc charge state envelopes in the m/z space permits the isolation of a single charge state of each polypeptide chain or the isolation of multiple charge states of the same polypeptide chain without co-isolation with the other chain. Avoiding co-isolation is important for successful fragmentation of a single species, generating non-chimeric spectra, which are subsequently easier to correctly interpret and match against the polypeptide primary chain sequence. A single charge state of the Lc chain was quadrupole-isolated using a 20 Th window and fragmented by HCD, CID, ETD, and

UVPD. MS/MS data were acquired for only three minutes in each dissociation method, and Lc graphical fragmentation maps were generated using TDValidator (Supplementary Figure S3). The combination of all the quickly acquired dissociation maps (resulting from 12 minutes. total instrument time) yielded 65% sequence coverage for Lc (Figure 3A). For Hc, multiple charge states were isolated in a 100 Th isolation window, and ions were fragmented using HCD, CID, ETD, and EThcD (Supplementary Figure S4). Acquisition time was comparable to the one needed for the Lc, and the combination of fragmentation maps resulted in 34.4% of sequence coverage for the most abundant proteoform Hc G1F (Figure 3B). No changes in the fragmentation maps were observed considering G0F or G2F glycans.

FAIMS-MS/MS was capable of separation and analysis of a mixture of reduced Lc and Hc from mAb in an unprecedented, easy, and fast fashion without the use of liquid chromatography or any other liquid fractionation technique. All fragmentation data obtained correspond to a minimum of four regular LC-MS/MS runs which would take around 10-15 minutes each, totaling 40-60 minutes of analysis not considering loading times, blanks, washes, and standards. The FAIMS-MS/MS method presented here required only 24 minutes to acquire all fragmentation data on Lc or Hc using 4 different dissociation methods, which is 40-60% faster than regular LC-MS/MS analysis. Further improvements in the acquisition routine can make the method even faster for the characterization of mAb and mAb conjugates. In this work, samples were manually sprayed, and data was acquired directly from Tune (instrument controller software). However, it is possible to use automated nanospray or microspray to run FAIMS-MS/MS in a high throughput manner far simpler than current LC-MS/MS analyses. The analysis of mAbs is a growing field that attracts the attention of many researchers and biopharmaceutical companies, and the new FAIMS-MS/MS method presented can improve speed, limit artefacts, and reduce costs of middle-down mAb analysis.

Abbreviations

mAb Monoclonal Antibody

IgGs Immunoglobulins G

Lc Light Chain

Hc Heavy Chain

FDA Food and Drug Administration

MS Mass Spectrometry

LC-MS/MS Liquid Chromatography Tandem Mass Spectrometry

S/N Signal to Noise

MS/MS Tandem Mass Spectrometry

RP Reverse Phase

SEC Size Exclusion

IEX Ion Exchange

FAIMS High-field asymmetric waveform ion mobility spectrometry

DC Direct Current

CV Compensation Voltage

TECP-HCl (2-carboxyethyl)phosphine Hydrochloride

AGC Automatic Gain Control

CID Collision Induced Dissociation

DV Dispersion Voltage

HCD Higher-energy Collisional Dissociation

NCE Normalized Collision Energy

UVPD Ultraviolet Photodissociation

ETD Electron Transfer Dissociation

EThcDElectron-transfer/Higher-energy Collision Dissociation

Hex Hexose

PTMs Post-translational Modifications

Acknowledgments

This research was carried out in collaboration with the National Resource for Translational and Developmental Proteomics under Grant P41 GM108569 from the National Institute of General Medical Sciences (NLK) and supported by the Sherman Fairchild Foundation. LF would like to thank the University of Oklahoma, Department of Biology, for start-up funds

Disclosure of potential conflicts of interest

KS and RH are Thermo Fisher Scientific employees, and NLK declares a COI with Proteinaceous.

Bibliography (max 50 references)

1. Beck A, Wagner-Rousset E, Ayoub D, Van Dorsselaer A, Sanglier-Cianferani S. 2013. Characterization of therapeutic antibodies and related products. *Anal Chem.* 85(2):715-736.
2. Kaplon H, Reichert JM. 2019. Antibodies to watch in 2019. *MAbs.* 11(2):219-238.
3. Beck A, Wurch T, Bailly C, Corvaia N. 2010. Strategies and challenges for the next generation of therapeutic antibodies. *Nat Rev Immunol.* 10(5):345-352.
4. Singh S, Kumar NK, Dwiwedi P, Charan J, Kaur R, Sidhu P, Chugh VK. 2018. Monoclonal antibodies: A review. *Curr Clin Pharmacol.* 13(2):85-99.
5. Fornelli L, Ayoub D, Aizikov K, Beck A, Tsybin YO. 2014. Middle-down analysis of monoclonal antibodies with electron transfer dissociation orbitrap fourier transform mass spectrometry. *Anal Chem.* 86(6):3005-3012.
6. Mukherjee R, Adhikary L, Khedkar A, Iyer H. 2010. Probing deamidation in therapeutic immunoglobulin gamma (igg1) by 'bottom-up' mass spectrometry with electron transfer dissociation. *Rapid Commun Mass Sp.* 24(7):879-884.
7. Tsybin YO, Fornelli L, Stoermer C, Luebeck M, Parra J, Nallet S, Wurm FM, Hartmer R. 2011. Structural analysis of intact monoclonal antibodies by electron transfer dissociation mass spectrometry. *Anal Chem.* 83(23):8919-8927.
8. Fornelli L, Damoc E, Thomas PM, Kelleher NL, Aizikov K, Denisov E, Makarov A, Tsybin YO. 2012. Analysis of intact monoclonal antibody igg1 by electron transfer dissociation orbitrap ftms. *Mol Cell Proteomics.* 11(12):1758-1767.
9. Mao Y, Valeja SG, Rouse JC, Hendrickson CL, Marshall AG. 2013. Top-down structural analysis of an intact monoclonal antibody by electron capture dissociation-fourier transform ion cyclotron resonance-mass spectrometry. *Anal Chem.* 85(9):4239-4246.
10. Fornelli L, Ayoub D, Aizikov K, Liu XW, Damoc E, Pevzner PA, Makarov A, Beck A, Tsybin YO. 2017. Top-down analysis of immunoglobulin g isotypes 1 and 2 with electron transfer dissociation on a high-field orbitrap mass spectrometer. *J Proteomics.* 159:67-76.
11. He L, Anderson LC, Barnidge DR, Murray DL, Hendrickson CL, Marshall AG. 2017. Analysis of monoclonal antibodies in human serum as a model for clinical monoclonal gammopathy by use of 21 tesla ft-icr top-down and middle-down ms/ms. *J Am Soc Mass Spectrom.* 28(5):827-838.
12. Szrentic K, Fornelli L, Laskay UA, Monod M, Beck A, Ayoub D, Tsybin YO. 2014. Advantages of extended bottom-up proteomics using sap9 for analysis of monoclonal antibodies. *Anal Chem.* 86(19):9945-9953.
13. Cotham VC, Brodbelt JS. 2016. Characterization of therapeutic monoclonal antibodies at the subunit-level using middle-down 193 nm ultraviolet photodissociation. *Anal Chem.* 88(7):4004-4013.
14. Fornelli L, Szrentic K, Huguette R, Mullen C, Sharma S, Zabrouskov V, Fellers RT, Durbin KR, Compton PD, Kelleher NL. 2018. Accurate sequence analysis of a monoclonal antibody by top-down and middle-down orbitrap mass spectrometry applying multiple ion activation techniques. *Anal Chem.* 90(14):8421-8429.
15. Szrentic K, Nagornov KO, Fornelli L, Lobas AA, Ayoub D, Kozhinov AN, Gasilova N, Menin L, Beck A, Gorshkov MV et al. 2018. Multiplexed middle-down mass spectrometry as a method for revealing light and heavy chain connectivity in a monoclonal antibody. *Anal Chem.* 90(21):12527-12535.
16. Jin Y, Lin Z, Xu Q, Fu C, Zhang Z, Zhang Q, Pritts WA, Ge Y. 2019. Comprehensive characterization of monoclonal antibody by fourier transform ion cyclotron resonance mass spectrometry. *MAbs.* 11(1):106-115.
17. Rehder DS, Dillon TM, Pipes GD, Bondarenko PV. 2006. Reversed-phase liquid chromatography/mass spectrometry analysis of reduced monoclonal antibodies in pharmaceuticals. *J Chromatogr A.* 1102(1-2):164-175.
18. von Pawel-Rammingen U, Johansson BP, Bjorck L. 2002. Ides, a novel streptococcal cysteine proteinase with unique specificity for immunoglobulin g. *EMBO J.* 21(7):1607-1615.

19. Sjogren J, Olsson F, Beck A. 2016. Rapid and improved characterization of therapeutic antibodies and antibody related products using ides digestion and subunit analysis. *Analyst*. 141(11):3114-3125.
20. Liu H, Gaza-Bulsecu G, Chumsae C. 2009. Analysis of reduced monoclonal antibodies using size exclusion chromatography coupled with mass spectrometry. *J Am Soc Mass Spectrom*. 20(12):2258-2264.
21. Hong P, Koza S, Bouvier ES. 2012. Size-exclusion chromatography for the analysis of protein biotherapeutics and their aggregates. *J Liq Chromatogr Relat Technol*. 35(20):2923-2950.
22. Fekete S, Beck A, Fekete J, Guillarme D. 2015. Method development for the separation of monoclonal antibody charge variants in cation exchange chromatography, part i: Salt gradient approach. *J Pharm Biomed Anal*. 102:33-44.
23. Fekete S, Beck A, Veuthey JL, Guillarme D. 2015. Ion-exchange chromatography for the characterization of biopharmaceuticals. *J Pharm Biomed Anal*. 113:43-55.
24. Prasad S, Belford MW, Dunyach JJ, Purves RW. 2014. On an aerodynamic mechanism to enhance ion transmission and sensitivity of faims for nano-electrospray ionization-mass spectrometry. *J Am Soc Mass Spectrom*. 25(12):2143-2153.
25. Purves RW, Prasad S, Belford M, Vandenberg A, Dunyach JJ. 2017. Optimization of a new aerodynamic cylindrical faims device for small molecule analysis. *J Am Soc Mass Spectrom*. 28(3):525-538.
26. Buryakov IA, Krylov EV, Nazarov EG, Rasulev UK. 1993. A new method of separation of multi-atomic ions by mobility at atmospheric-pressure using a high-frequency amplitude-asymmetric strong electric-field. *Int J Mass Spectrom*. 128(3):143-148.
27. Guevremont R. 2004. High-field asymmetric waveform ion mobility spectrometry: A new tool for mass spectrometry. *J Chromatogr A*. 1058(1-2):3-19.
28. Cooper HJ. 2016. To what extent is faims beneficial in the analysis of proteins? *J Am Soc Mass Spectrom*. 27(4):566-577.
29. Shvartsburg AA, Bryskiewicz T, Purves RW, Tang K, Guevremont R, Smith RD. 2006. Field asymmetric waveform ion mobility spectrometry studies of proteins: Dipole alignment in ion mobility spectrometry? *J Phys Chem B*. 110(43):21966-21980.
30. Shvartsburg AA. 2014. Ultrahigh-resolution differential ion mobility separations of conformers for proteins above 10 kda: Onset of dipole alignment? *Anal Chem*. 86(21):10608-10615.
31. Shvartsburg AA, Andrzejewski R, Entwistle A, Giles R. 2019. Ion mobility spectrometry of macromolecules with dipole alignment switchable by varying the gas pressure. *Anal Chem*.
32. Hebert AS, Prasad S, Belford MW, Bailey DJ, McAlister GC, Abbatiello SE, Huguet R, Wouters ER, Dunyach JJ, Brademan DR et al. 2018. Comprehensive single-shot proteomics with faims on a hybrid orbitrap mass spectrometer. *Anal Chem*. 90(15):9529-9537.
33. Marty MT, Baldwin AJ, Marklund EG, Hochberg GK, Benesch JL, Robinson CV. 2015. Bayesian deconvolution of mass and ion mobility spectra: From binary interactions to polydisperse ensembles. *Anal Chem*. 87(8):4370-4376.
34. Dong Q, Liang Y, Yan X, Markey SP, Mirokhin YA, Tchekhovskoi DV, Bukhari TH, Stein SE. 2018. The nistmab tryptic peptide spectral library for monoclonal antibody characterization. *MAbs*. 10(3):354-369.
35. Formolo T, Ly M, Levy M, Kilpatrick L, Lute S, Phinney K, Marzilli L, Brorson K, Boyne M, Davis D et al. 2015. Determination of the nistmab primary structure. State-of-the-art and emerging technologies for therapeutic monoclonal antibody characterization volume 2 biopharmaceutical characterization: The nistmab case study. American Chemical Society. p. 1-62.
36. Prien JM, Stockmann H, Albrecht S, Martin SM, Varatta M, Furtado M, Hosselet S, Wang MY, Formolo T, Rudd PM et al. 2015. Orthogonal technologies for nistmab n-glycan structure elucidation and quantitation. *Acs Sym Ser*. 1201:185-235.

37. Chen CH, Feng HT, Guo R, Li PJ, Laserna AKC, Ji Y, Ng BH, Li SFY, Khan SH, Paulus A et al. 2018. Intact nist monoclonal antibody characterization-proteoforms, glycoforms-using ce-ms and ce-lif. *Cogent Chem.* 4(1).

Figures legends

Figure 1. Mass spectra of reduced mAb (obtained from NIST) for two different settings of the FAIMS compensation voltage (CV) compared to no FAIMS. Spectra from direct injection (no FAIMS) of the mixture containing reduced light (Lc) and heavy (Hc) chains with the resultant spectra displayed in the m/z domain (A) and the deconvoluted spectra in the mass domain (B). Spectra obtained using FAIMS and applying -20 V of CV and displayed in the m/z domain (C) or deconvoluted into the mass domain (D) spectra. Spectra obtained using FAIMS and applying +40 V of CV and displayed in the m/z domain (E), or deconvoluted into the mass domain (F).

Figure 2. Expanded section of deconvoluted spectrum of light (Lc) and heavy (Hc) chains. Spectra obtained applying -20 V and +40 V of CV were deconvoluted and zoomed-in to show Lc (A) and Hc (B) proteoforms. Sodium adducts (+22 Da) are represented by a circle (●) and guanidine adducts (+60 Da) by a star (★). Addition of hexose (+162 Da) is characterized by +Hex and the loss of *N*-acetylglucosamine (-203 Da) as -GlcNAc.

Figure 3. Graphical fragmentation maps obtained from middle-down tandem MS of light (Lc) and heavy (Hc) chains. Cumulative fragmentation maps obtained from HCD, CID, ETD, and UVPD dissociation methods applied on Lc (A) and from HCD, CID, ETD, and EThcD applied to Hc (B). The red brackets represent *c*- and *z*- ions, blue brackets *b*- and *y*- ions, and green brackets *a*- and *x*- ions. The gray rectangle denotes a pyroglutamic acid post-translational modification and the orange rectangle the addition of the *N*-linked glycan G1F mass (the most abundant proteoform observed for the standard mAb obtained from NIST).

Figures

Figure 1

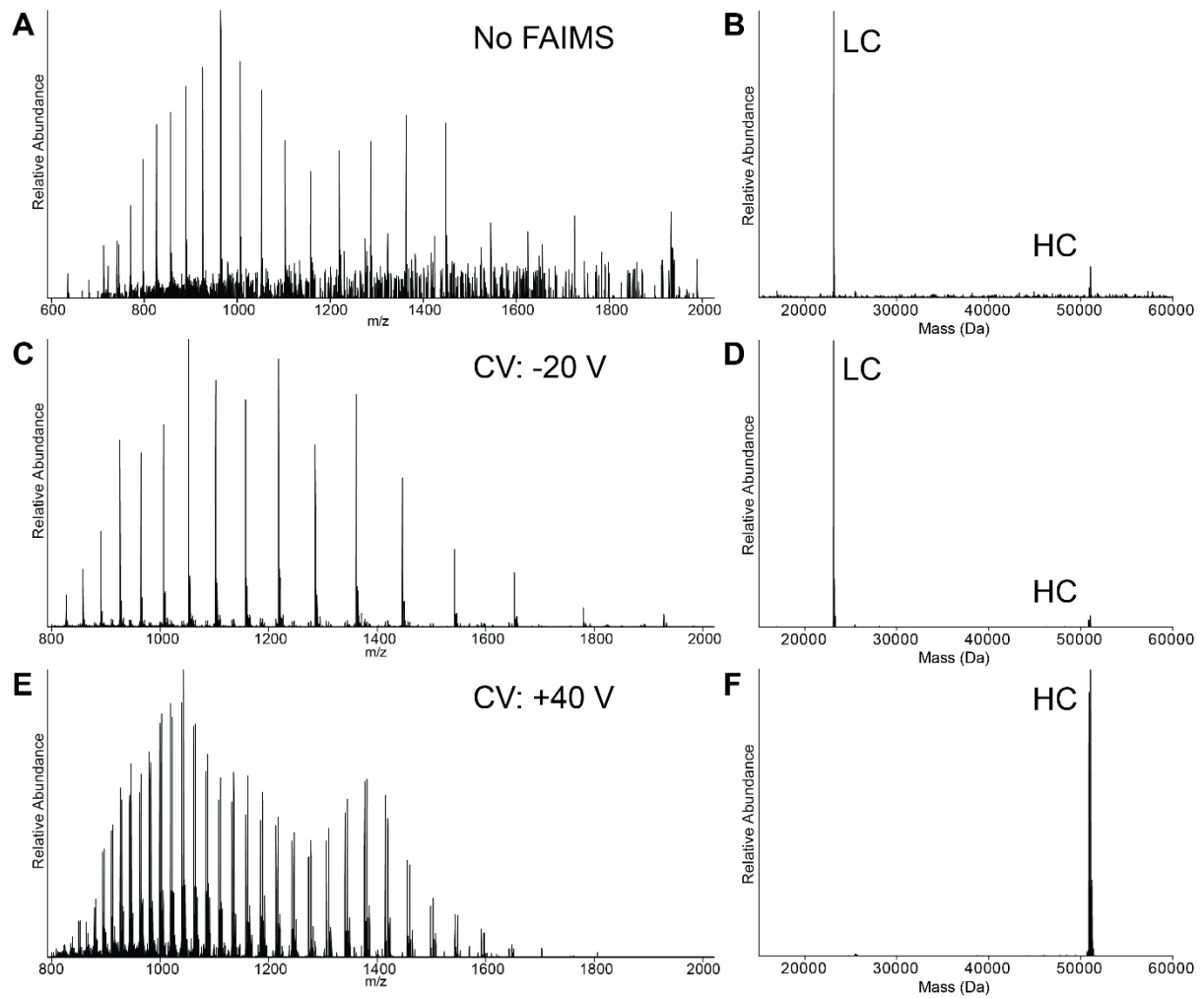


Figure 2

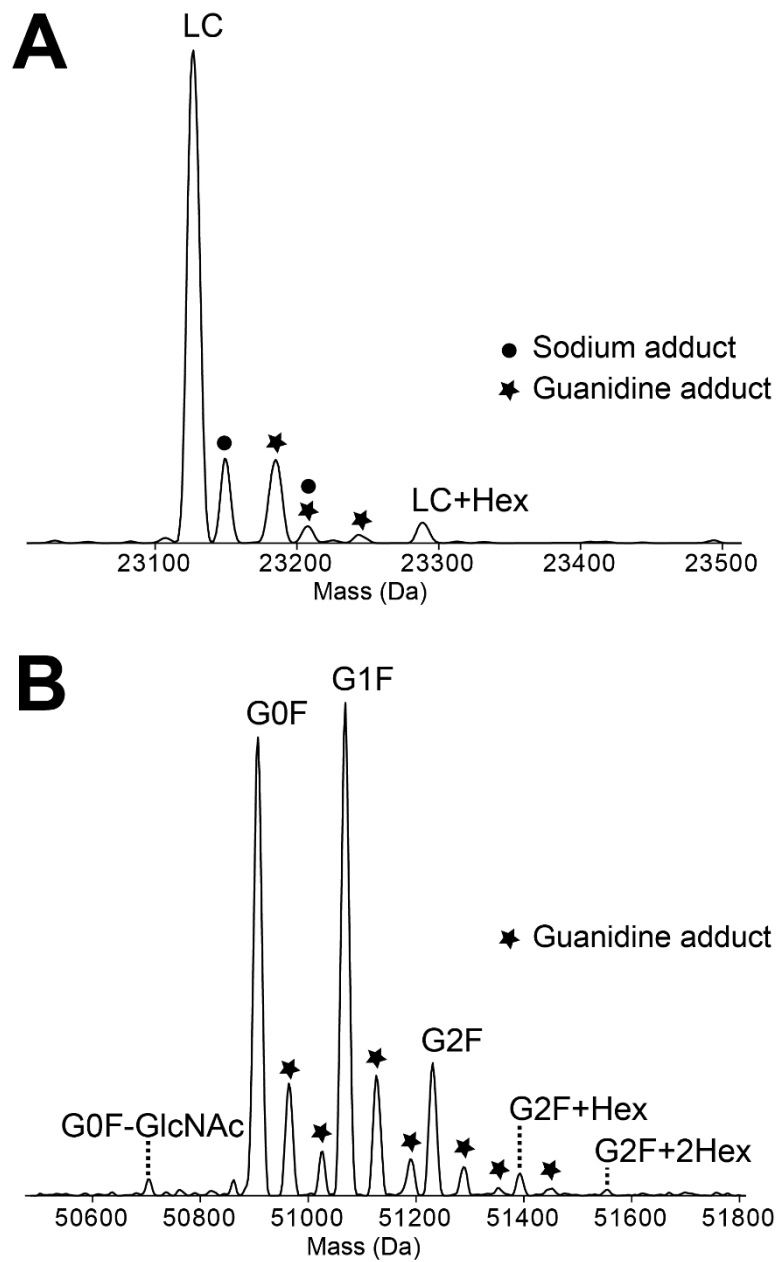


Figure 3

